Journal of Soil Sciences and Agricultural Engineering

Journal homepage: www.jssae.mans.edu.eg
Available online at: www.jssae.journals.ekb.eg

Generating The Electrical Energy from Sea Waves

El-Morsy, H. E.; Z. E. Ismail; R. G. Salim and A. M. Sherif*

Agric. Eng. Dept., Fac. of Agric., Mans. Univ.

ABSTRACT

The wide coverage and the untapped tremendous energy amount stored by the oceans makes the harness of ocean waves for electricity-generating is promising. Most techniques of wave energy converters (WECs) include a pneumatic or hydraulic interface between the wave converter and the electric generator for electricity-producing smoothly. But, a direct power take-off interface may be a way of increasing the capture and converting efficiency of wave power. This study was carried out to design, manufacture, performance analysis, and evaluation of capture and transforming wave energy efficiency for a new model of a single-axis wave energy converter (WEC) that extracts wave energy directly by a mechanical power take-off interface. Eventually, the study concluded that there is a specific configuration of the converter fits each wave condition for optimum performance that able to work by the efficiency of 10% to capture and convert the wave power. Also, the optimum performance for a selected place for installing the device should be performed starting at the design stage. One of the major condition in the design stage of the proposed WEC unit for the optimum performance is that the appropriate length of the WEC buoy (i.e., the length that is parallel to the wavelength propagation direction), should be designed with a length is equal or among (29.4 to 33.3 %) of the prevailing wavelengths.

Keywords: Wave energy converter, Capture efficiency, Single-axis, Power take-off interface.

INTRODCTION

The ocean waves carry tremendous energy amounts and if this energy could be captured for electricity production, it could make a great contribution to the global energy demand. From the beginning of the industrial revolution, global energy demand is in a continuous increase, and fossil fuel is the dominant source to meet that global demand. By contrast, this source is criticized for the greenhouse gases emission caused by human activities constantly for decades, in addition, the concerns about the depletion of this source (Hidayatullah, *et al*., 2011). In general, the energy activities represent by far the greatest emissions source about 68% of the human activities, where the activity of electricity and heat generation is responsible for 42% of the yearly global emissions of carbon dioxide from fuel combustion. Also, the emissions caused specifically from the electricity generation increased about 45% between 2000 and 2015 (IEA, 2017). If we have a chance to decrease these emissions, major modifications should be made in the electricity systems. Also, with the growth of environmental consciousness, the developed countries are becoming more desired to implant the policies of clean alternative energy for the sensitization in reducing the polluting emissions and find clean energy sources that could share in meeting the constantly growing global energy demand.

In the context of waves energy (Zhang, 2003) mentioned that harness of ocean waves for extracting energy is an old idea. Where the world's first wave energy device patent was registered in 1799 by Girard, in Paris. Moreover, the techniques developed with the aim of absorbing the energy from ocean waves and converting it into electricity are commonly called wave energy converters (WECs). In general, Thakare, *et al*. (2019) illustrated that harness of ocean waves for power generating is promising where the oceans cover around 70% of the earth's surface, which permits to access widely across the world and areas that are difficult to feed by electricity, like small islands that depend mostly on solar or wind power. Moreover, the entire world could be provided by sufficient power, in case of harness 0.2% of the ocean's untapped energy.

Despite the presented chances, the wave resources provided by neighboring oceans are barely being used; where Dellinger, (2015) mentioned that the marine energy technologies share by 0.01% of the electricity generation technology from renewable sources. One of the major challenges that facing wave energy technics was interpreted by (Ghosh and Prelas, 2011) that the contained energy amount by the oceans is tremendous and it can theoretically meet the global energy requirements more than many times; but practically, it is extremely difficult to harvest that enormous amount of energy economically for production widely. Where Leijon, *et al.* (2009) illustrated that these technologies economically, need strong finance for competing with the other renewable sources owing to the need for great infrastructure, need for over-dimensioning owing to the rare but frequent occurrences of harsh wave climate and the surviving ability for the parts exposed to the large ocean power, etc.

Generally, Holmberg, *et al.* (2011) and Ismail, (2014) suggested that there won't be one appropriate size for all solutions of converting wave energy, but only local wave conditions at the place of WEC device installation

* **Corresponding author.**
E-mail address: a.sherif92@yahoo.com
DOI: 10.21608/jssae.2019.79577

such as water climate and depth can determine the most suitable size and technology for each location.

The main objective of this study is to design and manufacture a new model of a single-axis wave energy converter that extracts wave energy directly by a mechanical power take-off interface. Moreover, creating a wide range of wave conditions; by controlling in the wavemaker variables. Thence, test the WEC model performance and estimate its efficiency of capture and transforming the power in waves.

MATERIALS AND METHODS

Wave energy converter: design and working principle

The WEC model was designed and manufactured during the period from 2015 and 2017 at the Agricultural Engineering Department of the Mansoura University in Egypt. During the converter design, the major challenge was to design a mechanical power take-off (PTO) system that able to achieve the follows:

- Converting the wave energy into mechanical motion in only one direction in both cases of pitching up or downing the buoy with the passing of a crest or a trough respectively.
- Rotating this mechanical motion with high velocity for the electricity generation.
- System possibility for adding more than one unit with no effect of the unit movement on any one other.

Hence, the system can cope with the random variability in the wave characteristics and with the random effect on all units, in addition, making the motion more stability, speed and higher torque.

The converter model was designed as illustrated in figure (1) to achieve the above objectives. Generally, the working principle of the power take-off system in the designed WEC is depending on two main movements are the upward movement caused by the wave force influence that acts for pitching the floating buoy up, and the downward movement is owing to the buoy weight influence. In both movements, a torque is created on the oscillating lever arm of the buoy around the buoy rotational axis; and by the connecting arm, the buoy pitching motion is translated to linear motion for the rack gear. Thence, the rack motion is transported to a combined gear consists of a small gear meshed with the rack (i.e., pinion) and large gear meshed with the output gear (i.e., speed gear) as shown in Fig (1-A). Otherwise, the output gear contains a pawl and ratchet mechanism inside it; as demonstrated in Fig (1-B), this mechanism works on making the motion of output shaft in an only one-way direction. Further, because of existing these two different behaviors when going up or down, so the modality of mesh the rack with the pinion gear plays the major role of getting the desired motion direction. Table (1) indicates the standard specifications of gears included in the power take-off system of the designed model.

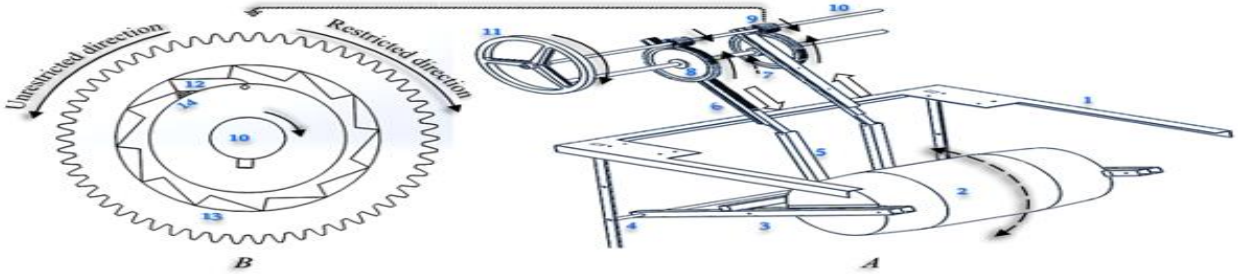

Figure 1. The main components schema of the designed wave energy converter
(A) Power take-off principle and (B) Pawl and ratchet mechanism inside the output gear

1.	**Tank frame**	**2.**	**Floating cylindrical buoy**	**3.**	**Lever arm**
4.	**Buoy rotational axis**	**5.**	**Connecting arm**	**6.**	**Rack gear**
7.	**Pinion gear**	**8.**	**Speed gear**	**9.**	**Output gear**
10.	**Output shaft**	**11.**	**Pulley**	**12.**	**Pawl**
13.	**Ratchet wheel**	**14.**	**Spring**		

Table 1. PTO Gears standard specifications

Gear Items	Module	Face width	Tip diameter	No. of tooth	Toothed length	Full length
Rack	0.9 mm	2 cm			45 cm	60 cm
Pinion	0.9 mm	2.5 cm	4.32 cm	46		
Speed	0.9 mm	2 cm	20.88 cm	230		
Output	0.9 mm	4 cm	5.04 cm	54		

Manufacture

Horizontal cylindrical buoy

Figure (2) shows the floating cylindrical buoy connected to the lever arm and connecting arms; where this cylindrical buoy is 33 cm in diameter, 60 cm wide and mass of 4.75 kg. The lever and connecting arms are an aluminum square bar with a length of 55.5 cm and 31 cm respectively.

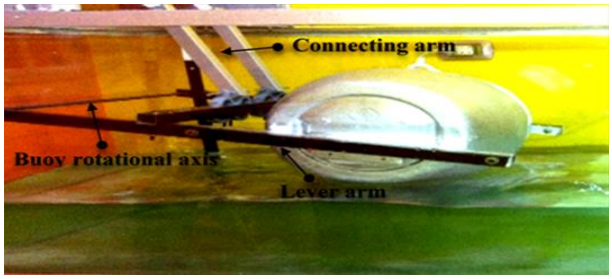

Figure 2. The buoy connected to the lever arm and connecting arms

Power take-off system

All gears were manufactured of MC polyamide Nylon material, owing to its properties such as the lightweight that was important for the model design suitability with the generated waves and the excellent resistance to organic chemicals that was quite good in this kind of environment for rustiness resistance. Otherwise, Fig (3-A) shows the installation of the PTO gears in the way that achieves the working principle objectives, while the pawl and ratchet mechanism inside the output gear shows in an internal view in Fig (3-B).

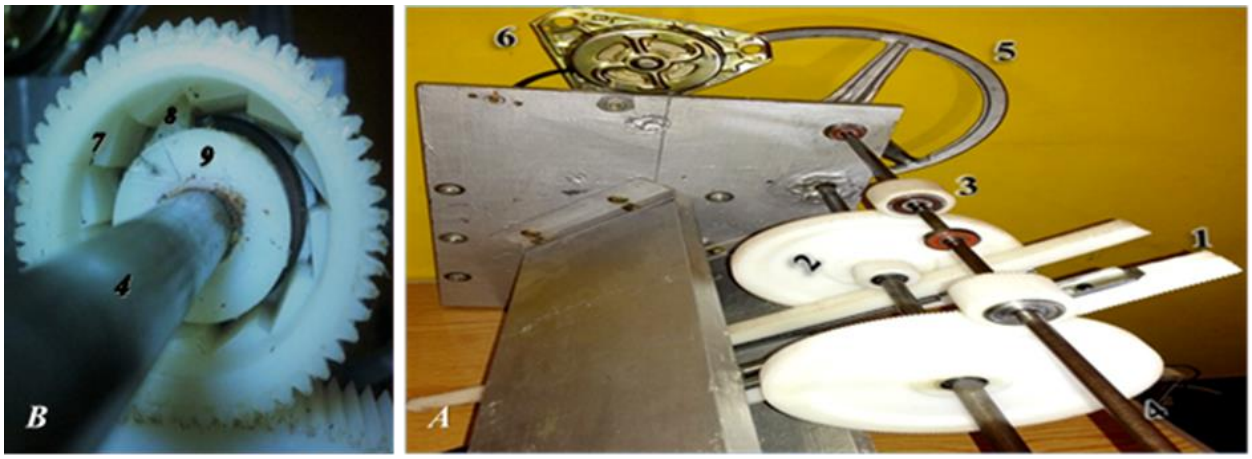

Figure 3. The main components of the designed wave energy converter

(A) Power take-off system and (B) Pawl and ratchet mechanism inside the output gear

1.	**Rack**	**2.**	**Combined gear**	**3.**	**Output gear**
4.	**Output shaft**	**5.**	**Pulley**	**6.**	**Generator**
7.	**Ratchet wheel**	**8.**	**Pawl**	**9.**	**Hub**

Scope of variables

In order to evaluate the proposed WEC model performance, a wide range of wave conditions had been created; by controlling in a flap-type wavemaker variables for getting different dimensions of wavelengths, wave heights. These variables are shown in figure (4) as follows:

- Flap stroke radius "r": 4.2; 6.9; 9.6 and 12.3 cm.
- Flap inclination angle "α": 80^o; 90^o; 100^o and 110^o.
- Inverter frequency supply that controls in the speed of wavemaker motor "f_s ": 2.8; 3.1 and 3.4 Hz.

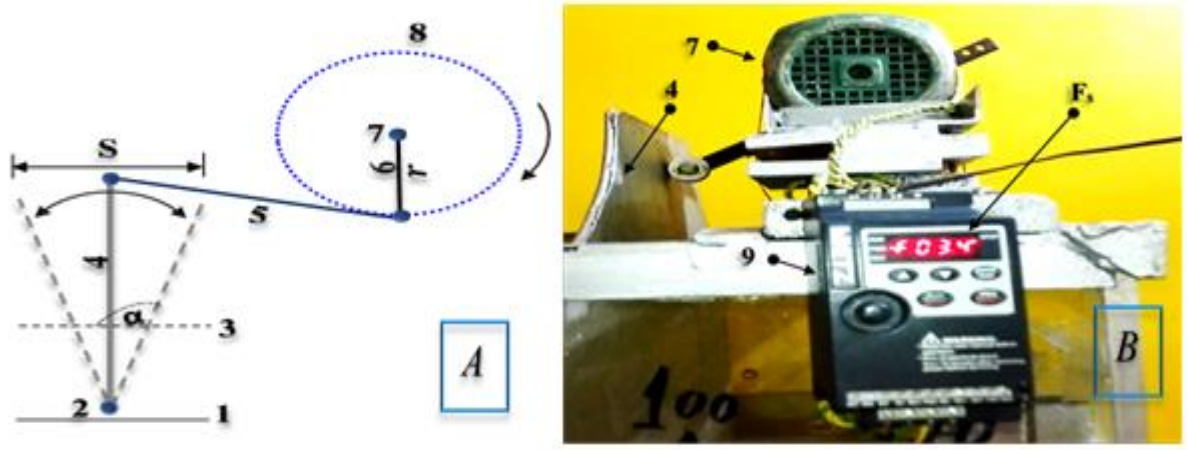

Figure 4. The main components of the wavemaker

(A) Schematic diagram and (B) Electric unit

1.	**Tank floor**	**2.**	**Pivot point**	**3.**	**Water level**	**4.**	**Hinged flap**
5.	**Connecting rod**	**6.**	**Crank**	**7.**	**Electric motor**	**8.**	**Crank circle**
9.	**Inverter**	**S.**	**Flap stroke**	**r.**	**Stroke radius**	**α.**	**Flap inclination angle**
f_s	**Inverter frequency supply**						

Measurements

Wave conditions

The wave dimensions that were measured are wavelength and wave height. While the wave parameter that was calculated is specific power in waves.

Wave height and length

In order to measure the wave height and length, a horizontal and vertical scale were drawn respectively on the side of the glass tank. Thence, these two dimensions were measured directly by observation, but the obtained values were taken and confirmed with the aid of photos and video sequences. One of these sequences is appreciated in figure (5).

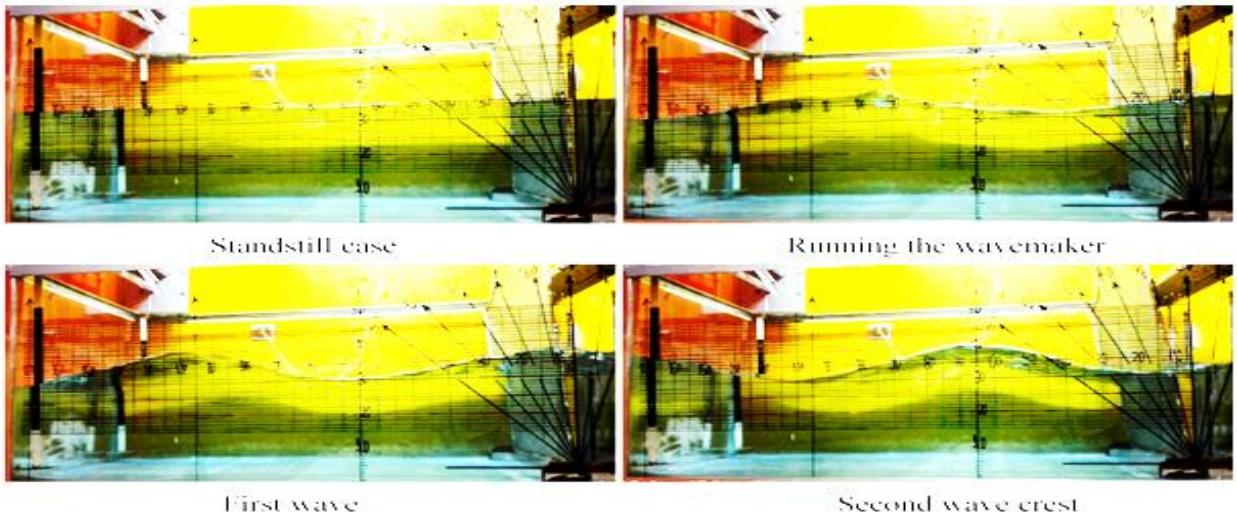

Figure 5. Sequence to measure main wave dimensions.

Specific wave power, (P_{wave})

The WEC was tested at a water depth of 35 cm. This depth has been compared to the obtained wavelengths. Where the results indicated that the waves at the water depth of 35 cm, is under the condition of transitional water waves. Hence, the specific power in wave per unit width (P_{wave}) was calculated according to the transitional water criteria and formulated in watt per meter as given by equation (1), (Alexandre, 2013):

$$P_{wave} = \frac{\rho g H^2}{32}(1+\tanh(kd))\left(\sqrt{\frac{g}{k}\tanh(kd)}\right)\left(1+\frac{2kd}{\sinh(2kd)}\right) \quad \ldots\ldots\ldots (1)$$

Where:

- (ρ) **is the density of water** [$1000\ Kg.m^{-3}$]
- (g) **is the gravitational acceleration** [$9.81\ m.sec^{-2}$]
- (H) **is the wave height** [m]
- (k) **is the wavenumber** [m^{-1}]
- (d) **is the water depth** [$0.35\ m$]

WEC performance

The performance evaluation of the wave energy converter was based on the output electric power from it, which was determined by multiplying the voltage by the electric current.

Extracted electric power, (P_{device})

Both the voltage and current output from the device generator was measured separately by using a Digital Multimeter. Since the values of these two parameters correlated directly with the rotational speed of the generator shaft and represent alternative current values, these values were altering almost every second. Therefore, the average of voltage and electric current readings was taken for a certain time depending on the aid of photos and video sequences. One of these sequences is appreciated in figure (6).

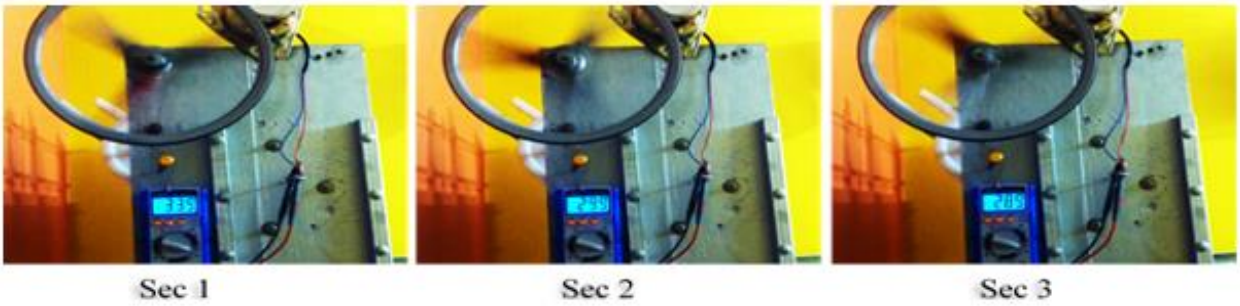

Figure 6. Sequence to measure the voltage.

WEC capture efficiency

Eventually, building upon measuring the electric power extracted by the device (P_{device}) and calculating the specific power of the wave per unit width (P_{wave}), the WEC capture efficiency was expressed as a percentage by applying the equation (2), (Price, *et al*., 2009):

$$\eta_c = \frac{P_{device}}{P_{wave} \cdot L_{device}} \ \% \quad \ldots\ldots\ldots\ldots (2)$$

Where:

- (η_c) **is the WEC capture efficiency**
- (P_{device}) **is the electric power extracted by the device** [$Watt$]
- (P_{wave}) **is the specific wave power per unit width** [$Watt/m$]
- (L_{device}) **is the width of the device** [$0.6m$]

RSULTS AND DISCUSSION

Wavelength

From the obtained data analysis, the wavelength (λ) is directly proportional to the flap stroke radius (r) where any increase in the stroke radius was giving significantly increase in wavelength; by contrast, it was in inverse relation with the increase of inverter frequency supply (□s). The shortest obtained wavelength was 0.68 m at the highest tested level of frequency supply (i.e., 3.4 Hz) and minimum tested length of stroke radius (i.e., 4.2 cm), while the longest obtained wavelength was 1.75 m at the lowest inverter frequency supply (i.e., 2.8 Hz) and maximum

tested length of stroke radius (i.e., 12.3 cm), as shown in Fig (7). Otherwise, the wavemaker failed to generate waves at the flap inclination angle of 80 degrees (α_1) with the stroke radius of 12.3 cm where these two variables together set the end of stroke at an inclination angle 60 degrees, where the flap at this position try to pull and generate the waves in the opposite direction when going back causing the wavemaker motor stopping.

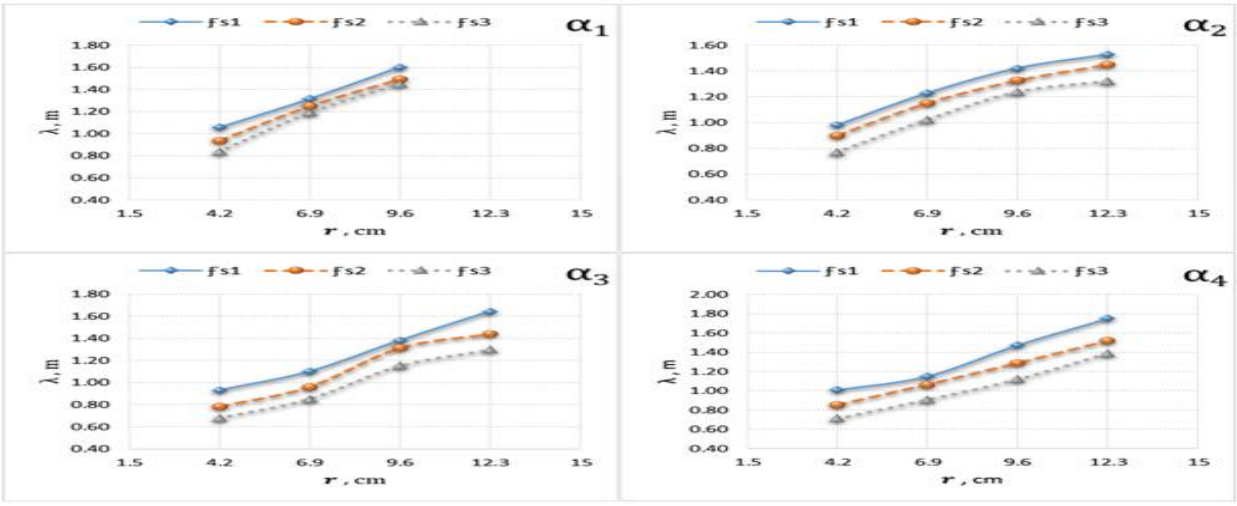

Figure 7. Effect of flap stroke radius on the wavelength dimension under the conditions of wavemaker variables

The average trend line for the four levels of flap stroke radius (r) for each inverter frequency supply ($\square_s$) indicated that the wavelength (λ) increases with the increase of flap inclination angle (α) more than 100 degrees or also with the decrease of flap inclination angle less than 100 degrees, which means that the shortest wavelengths can be obtained at inclination angle of 100 degrees compared to the wavelengths that can be obtained at another an inclination angles, as shown in figure (8).

The obtained data of the wavelength dimension was statistically analyzed by using Design-Expert® Software to explore the statistical significance of the wavemaker selected factors and estimate the regression coefficients to get the general correlation between the wavelength and the wavemaker variables. So, table (2) presents the ANOVA and regression coefficients as a quadratic regression model.

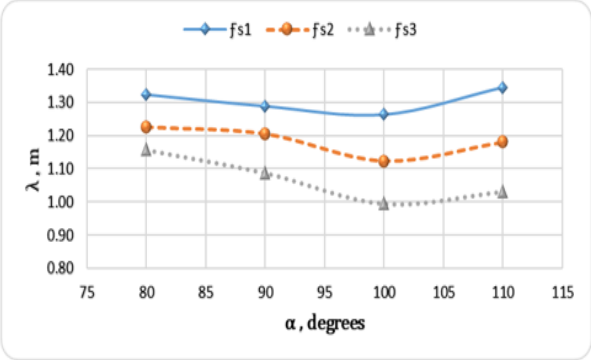

Figure 8. Effect of flap inclination angle on the wavelength dimension.

Table 2. Statistical analysis of the wavelength dimension.

Analysis of Variance					Regression Coefficients Confidence Intervals			
Source	**Sum of Squares**	**Mean Square**	**F.Value**	**P.Value**	**Coefficient**	**St. Error**	**95% C. L Low**	**95% C. L High**
Intercept	62.941	62.941			4.28983	2.043	0.14305	8.43672
Model	3.11	0.3455	133.38	< 0.0001*				
r	2.29	2.29	885.8	< 0.0001*	0.126356	0.044	0.03784	0.21486
α	0.1321	0.1321	50.97	< 0.0001*	-0.07764	0.017	-0.11283	-0.04245
$\square_s$	0.4209	0.4209	162.48	< 0.0001*	0.369689	1.144	-1.95213	2.69145
r · α	0.0004	0.0004	0.1512	0.6997	0.000105	0.0003	-0.00044	0.00065
r · $\square_s$	0.0011	0.0011	0.4185	0.5219	-0.006916	0.012	-0.02862	0.01478
α · $\square_s$	0.0218	0.0218	8.43	0.0064*	-0.00838	0.003	-0.01424	-0.00252
r^2	0.0085	0.0085	3.29	0.0783	-0.00197	0.001	-0.00417	0.00024
α^2	0.1086	0.1086	41.91	< 0.0001*	0.000513	10^{-4}	0.00035	0.00067
$\square_s^2$	0	0	0.0058	0.9395	0.013668	0.179	-0.34938	0.37673
Residual	0.0907	0.0026						
Total	3.2							

Building upon the obtained regression coefficients from the above statistical analysis, the general correlation between the wavelength dimension and the wavemaker terms was expressed by the following equation:

$$\lambda = 4.29 + 0.13r - 0.078\alpha + 0.37F_s + 0.0001r.\alpha - 0.007r.F_s - 0.008\alpha.F_s - 0.002r^2 + 0.0005\alpha^2 + 0.014F_s^2 \ldots\ldots\ldots (3)$$

Where, (λ) is the wavelength, m. (r) is the flap stroke radius, cm. (□$_s$) is the inverter frequency supply, (Hz) and (α) is the flap inclination angle, degrees.

The equation (3) can be used to make predictions about the wavelength dimension as much as possible at different operating points of the wavemaker variables, where the adjusted R^2 for this regression is 0.9644. Moreover, the flap stroke end shouldn't reach an inclination angle of 60 degrees for the reason indicated above, knowing that the change of stroke radius level changes the stroke end with an angle of 5 degrees, in addition, the levels of wavemaker variables in this equation should be specified in the original units cited above. Otherwise, the obtained actual values of the wavelength versus the predicted values by equation (3) at the same different operating points of the wavemaker variables, were shown in figure (9).

Wave height

The increase of flap stroke radius (r) led to an increase in wave height (H) even the second level value of stroke radius variable (r_2=6.9 cm); thereafter the wave height dimension decreased continuously with the increase of stroke radius values. On the other hand, it increased directly and continuously with the increase of inverter frequency supply value, as shown in figure (10). Also, at the flap inclination angle of 80 degrees (α1) with the stroke radius of 12.3 cm, the wavemaker failed to generate waves for the motor stop.

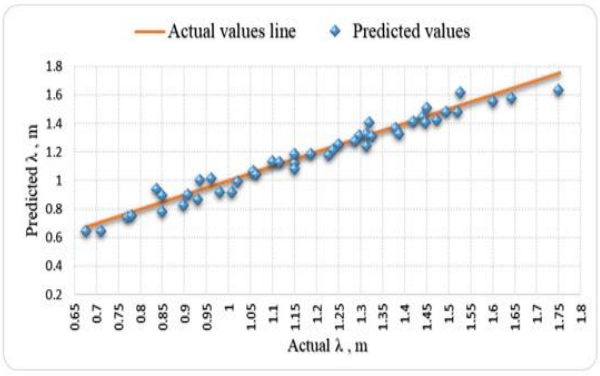

Figure 9. Actual values vs predicted regression values of the wavelength dimension.

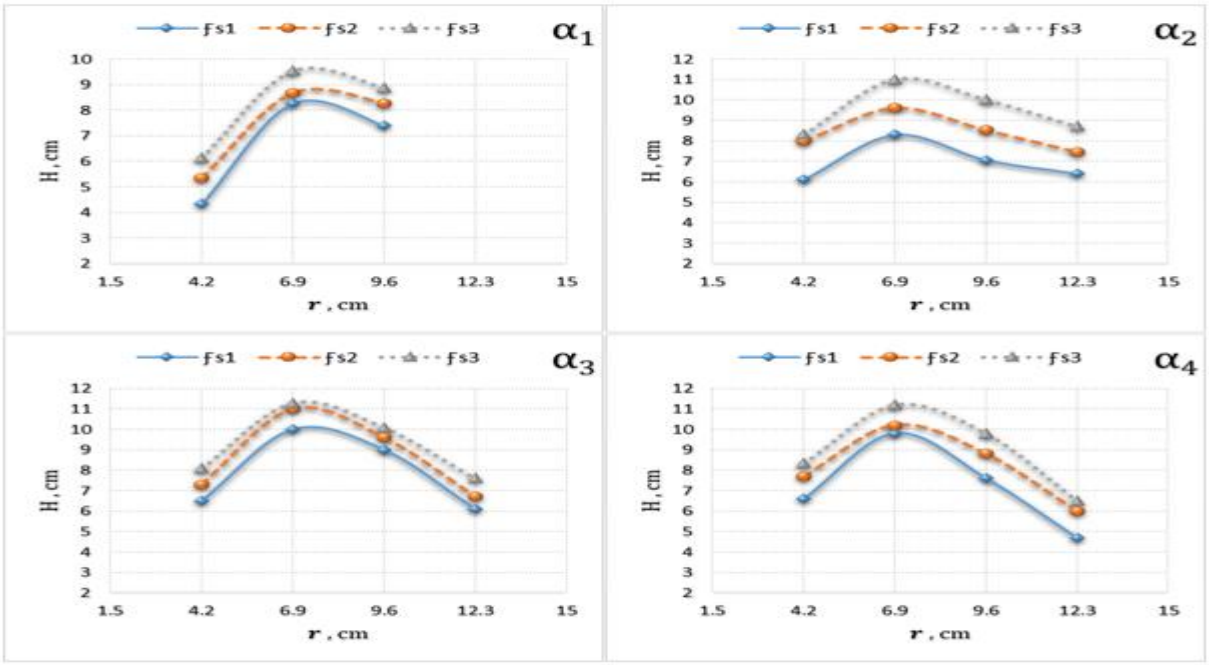

Figure 10. Flap stroke radius effect on the wave height dimension under the conditions of wavemaker variables

The average trend line for the four levels of flap stroke radius (r) for each inverter frequency supply (□$_s$), as shown in figure (11) indicated that the wave height decreases with the increase of flap inclination angle (α) more than 100 degrees or also with the decrease of flap inclination angle less than 100 degrees.

The obtained data of the wave height dimension was statistically analyzed by using Design-Expert® Software to explore the statistical significance of the wavemaker selected factors and estimate the regression coefficients to get the general correlation between the wave height and the wavemaker variables. So, table (3) presents the ANOVA and regression coefficients as a quadratic regression model.

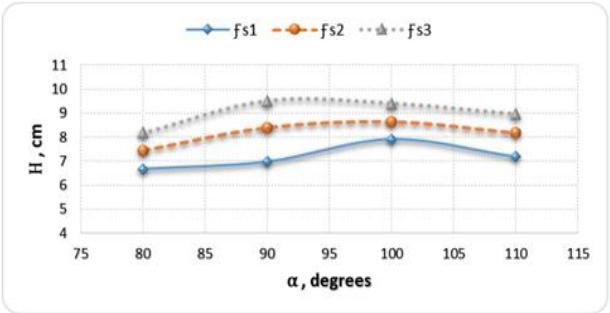

Figure 11. Effect of flap inclination angle on the wave height dimension

Table 3. Statistical analysis of the wave height dimension

Analysis of Variance					Regression Coefficients Confidence Intervals			
Source	**Sum of Squares**	**Mean Square**	**F.Value**	**P.Value**	**Coefficient**	**St. Error**	**95% C. L Low**	**95% C. L High**
Intercept	2989.38	2989.38			-73.40261	24.494	-123.1273	-23.6776
Model	119.17	13.24	35.55	< 0.0001*				
r	2.30	2.30	6.17	0.0179*	3.78723	0.523	2.7259	4.8486
α	5.17	5.17	13.89	0.0007*	0.96394	0.208	0.54199	1.3859
f_s	24.56	24.56	65.94	< 0.0001*	10.49859	13.714	-17.342	38.339
r · α	4.01	4.01	10.78	0.0023*	-0.010586	0.003	-0.017131	-0.00404
r · f_s	0.0185	0.0185	0.0497	0.8248	0.028590	0.128	-0.23166	0.288844
α · f_s	0.0460	0.0460	0.1235	0.7274	-0.012164	0.035	-0.082432	0.05811
r^2	70.28	70.28	188.66	< 0.0001*	-0.178946	0.013	-0.2054	-0.1525
α^2	7.42	7.42	19.93	< 0.0001*	-0.004240	0.001	-0.006168	-0.002312
f_s^2	0.0899	0.0899	0.2414	0.6262	-1.05372	2.144	-5.4072	3.29976
Residual	13.04	0.3725						
Total	132.21							

Building upon the obtained regression coefficients from the above statistical analysis, the general correlation between the wave height and the wavemaker terms was expressed by the following equation:

$$H = -73.4 + 3.8r + 0.96\alpha + 10.5f_s - 0.011r.\alpha + 0.03r.f_s - 0.012\alpha.f_s - 0.179r^2 - 0.0042\alpha^2 - 1.05f_s^2 \quad \ldots\ldots\ldots\ldots(4)$$

Where, (H) is the wave height, cm, (r) is the flap stroke radius, cm, (f_s) is the inverter frequency supply, (Hz) and (α) is the flap inclination angle, degrees.

The equation (4) can be used to make predictions about the wave height dimension as much as possible at different operating points of the wavemaker variables, where the R^2 of this regression is 0.9014. Moreover, the flap stroke end shouldn't reach an inclination angle of 60 degrees, in addition, the levels of wavemaker variables in this equation should be specified in the original units cited above. Furthermore, the obtained actual values of the wave height versus the expected values by equation (4) at the same different operating points of the wavemaker variables, were shown in figure (12).

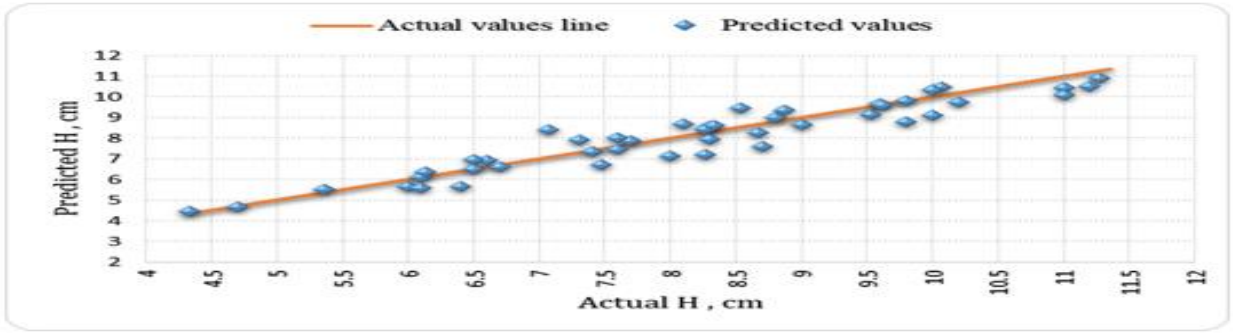

Figure 12. Actual values vs predicted regression values of the wave height dimension

Extracted power, (P_{device})

The extracted electric power values by the device (P_{device}) increased significantly with the increase of the flap stroke radius even the second level value of this variable (r_2= 6.9 cm); where thereafter, the extracted power values decreased continuously with the increase of stroke radius values. Otherwise, the two trend lines that represented the third tested level of the inverter frequency supply variable in the graph of α3 and α4, indicated that the extracted power values increased continuously even the third level value of stroke radius. Which means that the converter performance at the third stroke radius under conditions of these selected variables, is better than its performance at the second stroke length under conditions of the same variables, as shown in figure (13).

Generally, the reasons for converter performance change are in essence correlated directly to the wave conditions. At the first flap stroke, short wavelengths and high frequencies were obtained and that wasn't fit the floating buoy diameter (i.e., diameter= 33 Cm) for giving it the time needed to its movement (i.e., upward and downward), so the rate of upward and downward was very slight. At the second flap stroke, the wavelengths and heights increased beside the decline of wave frequency appropriately where all of these helped to give the floating buoy its time to move upward and downward with very suitable rate. As for the decline of WEC performance with the increase in stroke radius length over 6.9 cm, the wavelengths increased and wave frequency decreased too much, so the floating buoy was steadying for a while at the wave trough or crest to receive another wave action. Regard the exception that occurred in the graph of α3 and α4 for the third frequency supply, is owing to the obtained wave dimensions were more appropriate to the converter design than the wave dimensions that generated at the second stroke radius under the same conditions of wavemaker variables.

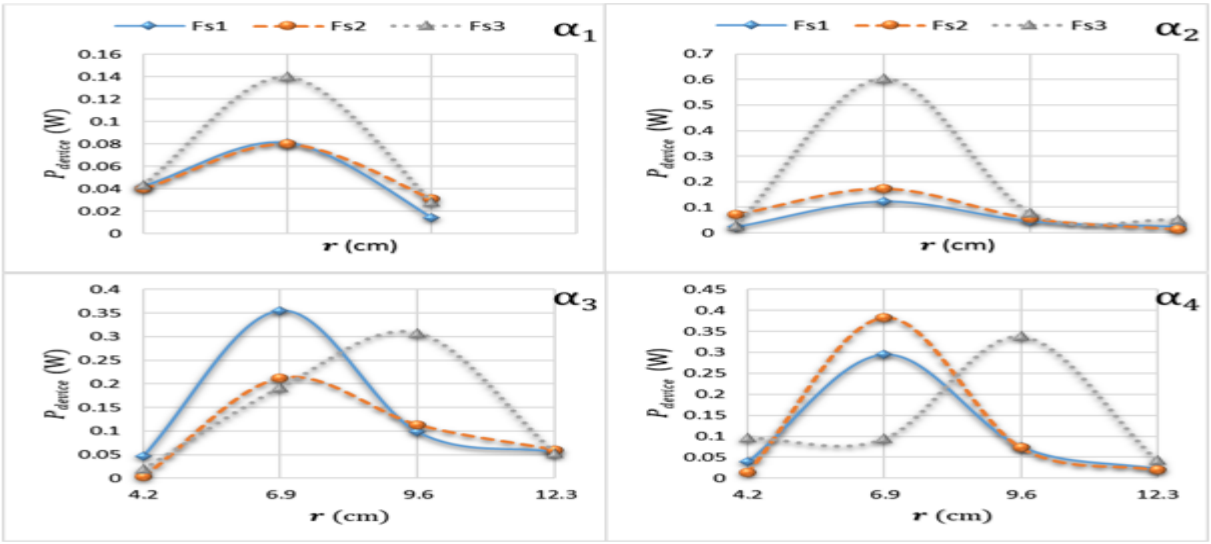

Figure 13. Flap stroke radius effect on the extracted electric power

Owing to the performance of the wave energy converter is depending directly on operating wave conditions. So, the main wave dimensions that are the most appropriate for the converter design and its highest performance, were set depending on analyzing the surface plots (i.e., diagram of three-dimensional data) and contour plots of all obtained data, as shown in figure (14). Where this analysis showed that the most appropriate wave dimensions for the model design were as follow:

- ✓ The wavelength is range from 100 to 113 cm (i.e., $3 \leq \lambda \geq 3.4$ times buoy diameter).
- ✓ The wave height is range from 9 to 13 cm

Where, the converter performance in the formed wave conditions from the values of these dimensions, is able to give an electric power starts from 0.4 to 0.63 Watt. Comparing to the specific wave power in these conditions, the converter works with a capture efficiency of 8 to 10 %.

Capture efficiency

The results expounded showed that with the availability of the appropriate wave conditions for the design, the device is able to work with a capture efficiency of 10%. In general, figure (15) shows the efficiencies that were captured by the device in the obtained different conditions of the extracted power and specific wave power; in addition to the proportional relationship between the capture efficiency and extracted power.

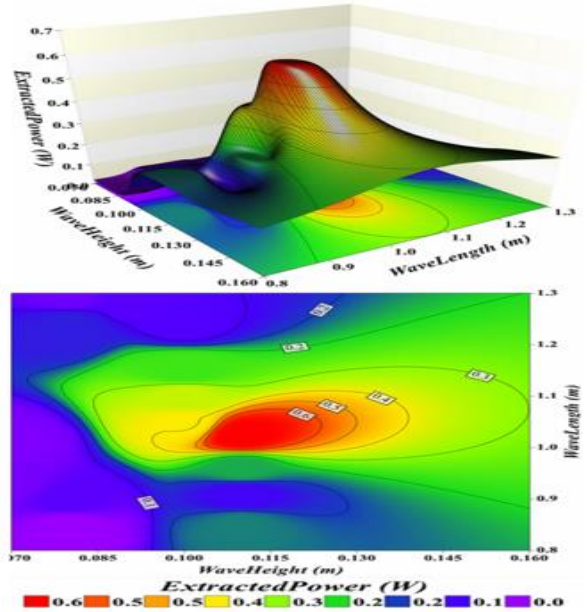

Figure 14. The surface and contour plots for the response of extracted electric power to the essential wave dimensions

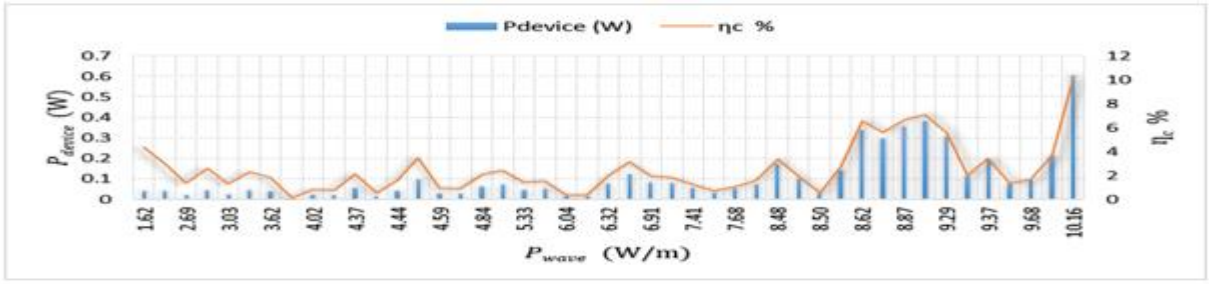

Figure 15. Capture efficiency vs extracted power and specific wave power

CONCLUSION

Eventually, the study concluded that there is a specific configuration of the converter fits each wave condition for optimum performance that able to work by the efficiency of 10% to capture and convert the wave power. So, the optimum performance for a selected place for installing the device should be performed starting at the design stage. One of the major condition in the design stage of the WEC unit for the optimum performance is that the appropriate length of the WEC buoy (i.e., the length

that is parallel to the wavelength propagation direction), should be designed with a length is equal or among (29.4 to 33.3 %) the prevailing wavelengths.

REFERENCES

Alexandre, A. (2013). Wave Energy Converter Strings for Electricity Generation and Coastal Protection. PhD dissertation. Manchester University, UK.

Dellinger, G. (2015). Etude expérimentale et optimisation des performances hydrauliques des vis d'Archimède utilisées dans les micro centrales hydroélectriques. PhD dissertation. University of Strasbourg.

Ghosh, T. K. and Prelas, M. A. (2011). Energy Resources and Systems - Volume 2: Renewable Resources. Springer-Dordrecht Heidelberg London New York. Vol.2 (5), pp.267-320. DOI 10.1007/978-94-007-1402-1. ISBN 978-94-007-1401-4.

Hidayatullah, N. A., B. Stojcevski. and A. Kalam. (2011). Analysis of distributed generation systems, smart grid technologies and future motivators influencing change in the electricity sector. Scientific Research. Vol. 2, pp. 216-229.

Holmberg, P., M. Andersson., B. Bolund. and K. Strandanger. (2011). Wave Power - Surveillance study of the development. Elforsk.

IEA., International Energy Agency. (2017). CO2 emissions from fuel combustion - highlights (2017 Edition). OECD/IEA, Paris, France.

Ismail, Z. E. (2014). Basics of Power and Machinery in Agricultural Engineering- (2nd edition). researchgate.net.

Leijon, M., R. Waters., M. Rahm., O. Svensson., C. Boström., E. Strömstedt., J. Engström., S. Tyrberg., A. Savin., H. Gravrakmo., H. Bernhoff., J. Sundberg., J. Isberg., O. Agren., O. Danielsson., M. Eriksson., E. Lejerskog., B. Bolund., S. Gustafsson. and K. Thorburn. (2009). Catch The Wave to Electricity - The Conversion of Wave Motion to Electricity Using a Grid-Oriented Approach. IEEE Power and Energy Magazine. Vol.7, no.1, pp.50-54. DOI: 10.1109/MPE.2008.930658.

Price, A. A. E., C. J. Dent. and A. R. Wallace. (2009). On the capture width of wave energy converters. Applied ocean research., 31 (4). pp. 251-259.

Thakare, J., S. Patil. and C. J. Sharma. (2019). Study of Generation of Electrical Energy from Ocean Waves. International Journal of Research in Electronics and Computer Engineering (IJRECE). Vol.7, pp. 2498- 2502. ISSN: 2348-2281.

Zhang, H. (2003). Ocean Electric Energy Extraction Opportunities. Master's Thesis. Oregon State University.

توليد الطاقة الكهربائية من أمواج البحر

حسني الشبراوي المرسى ، زكريا إبراهيم إسماعيل ، رضا جمعه سالم و أحمد محب شريف
قسم الهندسة الزراعية ـ كلية الزراعة ـ جامعة المنصورة

تتضمن معظم تقنيات محولات الطاقة الموجية (WECs) واجهة هوائية أو هيدروليكية بين محول الموجة او نقطة التقاط الموجات والمولد الكهربائي لإنتاج الكهرباء بسلاسة. ولكن، قد تكون واجهة التحويل المباشر للطاقة وسيلة لزيادة كفاءة التقاط وتحويل قدرة الموجة. أجريت هذه الدراسة لتصميم وتصنيع وتحليل الأداء وتقييم كفاءة التقاط وتحويل طاقة الأمواج لنموذج أولي جديد لمحول طاقة موجة أحادي المحور يستخرج طاقة الأمواج مباشرة من خلال واجهة تحويل قدرة ميكانيكية. أيضا، تحديد إمكانات نموذج المحول كنموذج حقيقي عند العمل في مكان محدد. لتحقيق اهداف الدراسة، تم تصميم وتصنيع نموذج محول طاقة الموجه في قسم الهندسة الزراعية بجامعة المنصورة في مصر بين عامي 2015 و2017 وتثبيته على حوض يتم به خلق مجموعه واسعه من الظروف الموجية بواسطة التحكم في متغيرات صانع موجات وهي أربعه اطوال لنصف قطر مشوار رفرف صانع الموجه" r" (4.2، 6.9، 9.6 و12.3 سم)، أربعه زاويا لميل الرفرف" α" (80، 90، 100 و110 درجة)، عرض تردد انفرتر التحكم في موتور صانع الموجه" f_s " (2.8، 3.1 و3.4 هرتز). ثم اجريت سلسلة من التجارب لدراسة عوامل صانع الموجه سابقه الذكر على ظروف الموجه من ابعاد رئيسيه هي الطول الموجي وارتفاع الموجه، ومن ثم تقييم سلوك وكفاءة المحول في تلك الظروف الموجية. لخصت هذه الدراسة، أن هناك تكوينًا محددًا للمحول يناسب كل حالة موجية للحصول على أداء مثالي قادر على العمل بكفاءة 10٪ لالتقاط وتحويل طاقة الموجة. لذلك، يجب إجراء الأداء الأمثل للمكان المحدد لتثبيت الجهاز بدءًا من مرحلة التصميم. أحد الشروط الرئيسية في مرحلة تصميم وحده المحول للأداء الأمثل هو أن الطول المناسب للعوامة المستخدمة او بشكل عام طول نقطه التقاط طاقة الأمواج الموازي لاتجاه انتشار الموجة يجب تصميمه بطول مساواً او يتراوح بين (29.4 الى 33.3 ٪) الاطوال الموجية السائدة.